Bidirectional Reflectance Distribution Function And Hemispherical Reflectance of JSC Mars-1

Georgi T. Georgiev[a], James J. Butler[b]

[a]Science Systems and Applications, Inc., Lanham, MD 20706, e-mail: gtg@spectral.gsfc.nasa.gov
[b]NASA Goddard Space Flight Center, Code 920.1, Greenbelt, MD 20771

ABSTRACT

Novel data are presented of Bidirectional Reflectance Distribution Function (BRDF) and 8° directional/hemispherical reflective measurements of Martian regolith simulant JSC Mars-1. The scatterometer of the National Aeronautics and Space Administration's Goddard Space Flight Center (NASA's GSFC) Diffuser Calibration Facility (DCaF) was used for the measurements reported. The data were obtained with a monochromator-based light source in the UltraViolet (UV), Visible (VIS), and Near InfraRed (NIR) spectral regions. The BRDF measurements were performed at different angles of incidence, and over a range of in-plane and out-of-plane geometries. The 8° directional/hemispherical reflective measurements were calibrated using a gray Spectralon sample set of 7 plates. The results presented are NIST traceable through calibrated standard plates. The hemispherical and diffuse scatter data obtained from these studies are important for future Mars space and ground based observations.

Keywords: Optical scattering, BRDF, Hemispherical reflectance, Reflectance spectroscopy, Polarization optics.

1. INTRODUCTION

The optical characterization of the reflectance of materials is usually performed by commercial spectrophotometers. Typical measurements are the directional and diffuse reflectance of the samples as a function of wavelength. To better investigate the optical properties of those samples, it is useful to know their bidirectional reflectance distribution function (BRDF) at different angles of incidence and scatter as well as their hemispherical reflectance.

We are presenting the results of BRDF and 8 degree directional/hemispherical reflective measurements of Martian regolith simulant JSC Mars-1 performed in the Diffuser Calibration Facility (DCaF) at NASA's Goddard Space Flight Center (GSFC). The facility scatterometer[1], located in a class 10,000 laminar flow cleanroom, is a fully automated instrument capable of measuring the BRDF of a wide range of sample types in the spectral range from 230nm to 900nm. The scatterometer can perform in-plane and out-of-plane BRDF measurements with typical measurement uncertainty of less than 1.0% (k = 1). Recently, the scatterometer measurement capabilities were expanded with a new reflectance sphere designed and built for 8° directional/hemispherical measurements in the UV, VIS and NIR spectral range. The uncertainty of the hemispherical measurements is less than 1.0% (k = 1) for the setup used. The scatterometer is regularly calibrated, and the results presented are traceable to measurement made on the National Institute of Standards and Technology's (NIST's) Special Tri-function Automated Reference Reflectometer (STARR)[2].

The JSC MARS-1 sample is the < 1 mm diameter fraction of weathered volcanic ash from Pu'u Nene, a cinder cone on the island of Hawaii, which has been repeatedly cited as a close spectral analog to the bright Mars regions[3]. The experimental data were obtained with the monochromator-based light source from 250 to 900 nm. The BRDF data were recorded at different angles of incidence and at in- and out-of-plane geometries. The 8° directional/hemispherical reflectance of the sample was also measured.

The reported data are intended to more completely describe the characteristics of JSC Mars - 1 Regolith Simulant through analysis of its diffuse reflectance properties. The sample exhibits a wide range of BRDF values depending on angle of incidence and scatter. The BRDF and hemispherical data are given for a spectral range from 250 to 900 nm for better understanding the material properties. The high quality of the data is supported by the fact the measurements were done in a clean room calibration facility and the results are NIST traceable.

2. BACKGROUND

As shown in Fig. 1, the BRDF is usually referred to as the ratio of the scattered radiance L_s scattered by a surface into the direction (θ_s, ϕ_s) to the collimated irradiance E_i incident on a unit area of the surface[4]:

$$BRDF = \frac{L_s(\theta_i, \phi_i, \theta_s, \phi_s, \lambda)}{E_i(\theta_i, \phi_i, \lambda)}, \tag{1}$$

where θ is the polar angle, ϕ is the azimuthal angle, the subscripts *i* and *s* are for the incident and scattered directions respectively, and λ is the wavelength. In practice, we usually present BRDF in terms of the incident power, scattered power and the geometry of the reflected scatter. It is equal to the scattered power per unit solid angle normalized by the incident power and the cosine of the detector view angle[5]:

$$BRDF = \frac{P_s / \Omega}{P_i \cos\theta_s}, \tag{2}$$

where P_s is the scatter power, Ω is the solid angle determined by the detector aperture, *A*, and the radius from the sample to the detector, *R*, or $\Omega = A/R^2$, P_i is the incident power, and θ_s is the scatter angle.

The 1.0% uncertainty specification of the measurement depends on several instrument variables[1]. The uncertainty in a BRDF measurement, Δ_{BRDF}, evaluated and expressed in accordance with NIST guidelines[6] is presented by

$$(\Delta_{BRDF})^2 = 2(\Delta_{NS})^2 + 2(\Delta_{LIN})^2 + (\Delta_{SLD})^2 + (\Delta_{\theta s} \tan(\theta_s))^2, \tag{3}$$

where Δ_{NS} is the noise to signal ratio, Δ_{LIN} is the non-linearity of the electronics, Δ_{SLD} is the error of the receiver view angle, $\Delta_{\theta s}$ is the error of the total scatter angle, and θ_s is the error of the receiver scatter angle. The error of the receiver view angle, Δ_{SLD}, can be further expressed by

$$(\Delta_{SLD})^2 = (2\Delta_{RM})^2 + (2\Delta_{RZ})^2 + (2\Delta_{RA})^2, \tag{4}$$

where Δ_{RM} is the error of the receiver arm radius due to the goniometer, Δ_{RZ} is the error of the receiver arm radius due to sample Z direction misalignment, and Δ_{RA} is the error of the receiver aperture radius. The total scatter angle error, $\Delta_{\theta s}$, can be expressed by

$$(\Delta_{\theta s})^2 = (\Delta_{\theta M})^2 + (\Delta_{\theta Z})^2 + (\Delta_{\theta T})^2, \tag{5}$$

where $\Delta_{\theta M}$ is the error of the scatter angle due to the goniometer, $\Delta_{\theta Z}$ is the error due to sample Z direction misalignment, and $\Delta_{\theta T}$ is the sample tilt error.

The 8° directional/hemispherical reflectance integrating sphere collects and spatially integrates the scattered optical radiation. The sphere interior is Spectralon with typical reflectance of 94% to 99% from the UV to the NIR. The sphere was designed with several ports to accommodate the sample, the detector, and the entry of the incident light. A fourth port is a spare and is typically closed using a Spectralon plug. The total port area is less than 5% of the total

surface area of the sphere. It is important to have the radiation balance inside the sphere established after as few internal reflections as possible. The light intensity incident on the detector should correspond to the average light intensity inside the sphere. An interior baffle is employed to block the detector viewing light reflected directly from the sample.

3. EXPERIMENTAL

Bidirectional reflectance distribution function: setup and measurement

We used the DCaF scatterometer to measure the in- and out-of-plane BRDF of the sample material. The measurements were performed at angles of incidence of 0^o, $\pm10^o$, 20^o, $\pm30^o$, 40^o, 50^o, $\pm60^o$ in-plane and at 0^o and $\pm10^o$, out-of-plane. The scatter data were collected at angles of 0^o, 10^o, 20^o, 30^o, 40^o, 50^o and 60^o. The light source was a 75 W Xenon lamp coupled to a Chromex 0.25m monochromator. The monochromatic light beam was mechanically chopped. Scattered light was detected using a silicon photodiode with output fed to a computer-controlled lock-in amplifier. For better characterization of the material scatter, data were collected from the UV into the NIR spectral range in 50 nm steps from 250 to 900 nm for the 0^o and $\pm10^o$ in plane and out-of-plane incident angles. Scatter data were collected in 100 nm steps for in-plane incidence angles of 30^o and 60^o and in 200 nm steps for in-plane incidence angles of 20^o, 40^o, 50^o, -30^o and -60^o. Two measurements, for S and P polarization of the incident beam, were made at each point and the unpolarized scatter is reported in this paper. The scatterometer was calibrated using NIST calibrated Spectralon and pressed halon samples. The optical setup of the instrument is shown in Fig.2. The JSC Mars-1 sample is shown in Fig.3 positioned on the sample stage.

BRDF at normal incidence

Fig. 4 shows the BRDF acquired at 0^o incidence from 250 to 900 nm in 50 nm steps and at scatter angles from -60^o to 60^o in 10 degree steps. The measured curves are given in Fig.4 for the in plane measurement. We also measured the BRDF at a 0^o incident/90^o out-of-plane configuration over the same spectral range at scatter angles of 0^o to 60^o in 10^o steps. These data are presented in Fig 5.

The results presented in Figs.4 and 5 are useful for understanding the BRDF properties of the material. The values are from $4.7x10^{-3}$ sr^{-1} at 250 nm to $73.7x10^{-3}$ sr^{-1} for 800 and 850 nm. The BRDF for 900 nm is a little bit lower and can be attributed to the ferric absorption band in the 800-900 nm region. The BRDF is symmetric at all wavelengths and scatter angles. Increased retro-scatter is particularly evident at the NIR wavelengths.

The out-of-plane measured data support similar conclusions. The BRDF curves in the UV, particularly at 250 and 300 nm, appear significantly flatter than those at higher wavelengths. It can be concluded from the values of the BRDF for both the in- and out-of-plane measurements that the material has a symmetric BRDF response in all scatter directions at normal incidence.

BRDF at non-normal angles of incidence

We measured the BRDF at 10^o incidence from 250 to 900 nm in 50 nm steps and at 30^o and 60^o incidence in 100 nm steps. The data were recorded at scatter angles from -60^o to 60^o in 10^o steps. The curves for the in-plane measurements at 10^o, 30^o and 60^o are given in Figs.6, 7 and 8, respectively. We also measured the 90^o out-of-plane BRDF at 10^o incidence from 250 to 900 nm in 50 nm steps over a scatter angle range of 0^o to 60^o in 10^o steps. These data are shown in Fig. 9.

The BRDF values at 250 nm and 60^o forward scatter range from $4.01x10^{-3}$ sr^{-1} at 10^o incident angle to $6.54x10^{-3}$ sr^{-1} at 60^o incident angle. The BRDF range from $57.39x10^{-3}$ sr^{-1} at 10^o incident angle to $60.74x10^{-3}$ sr^{-1} at 60^o incident angle at 900 nm and 60^o forward scatter. Strong optical back-scattering of the material is evident in these data. The back-scattering increases in average for all wavelengths measured. For example, the back-scatter at scatter angle of -20^o is

3.03% higher than those measured at scatter angle of 0^o for 10^o incident angle and at scatter angle of -40^o it is 8.27% higher than those measured at scatter angle of -20^o for 30^o incident angle. The shapes of the BRDF curves measured at all wavelengths show the same general diffuse reflectance behavior of the material at each scatter angle.

The out-of-plane data support similar conclusions. The BRDF curves in the UV, especially at 250 and 300 nm, are significantly flatter than those measured in the near infrared. The BRDF increases with increasing wavelength. In addition, the increasing BRDF is higher at lower scatter angles. It can be concluded from the BRDF values for in and out-of-plane measurements that the material has the same BRDF response behavior in all hemispherical directions for each scatter angle.

The BRDF in-plane data at -10^o of incidence is presented in Fig.10. We also measured BRDF in-plane at -30^o and -60^o and out-of-plane at -10^o angle of incidence. The conclusions we have from those measurements support the results from in plane -10^o and out-of-plane 10^o angle of incidence measurements.

The in-plane BRDF data at positive incident angles mirror those measured at negative angles for the same wavelengths and scatter angles. The back-scatter at scatter angle of 0^o is 3.41% higher than those measured at scatter angle of 20^o for -10^o incident angle and at scatter angle of 40^o it is 8.27% higher than those measured at scatter angle of 20^o for -30^o incident angle, which is in a good agreement with the corresponding values measured at positive angles of incidence. The shapes of the BRDF curves appear as mirror images of those measured at positive angles of incidence at identical wavelengths.

8 deg hemispherical setup and measurement

The 8 degree directional/hemispherical reflectance of JSC Mars-1 was measured at wavelengths of 300, 400, 500, 600, 700, 800 and 900 nm using the same monochromatic light source used in the BRDF measurements. The only hardware difference from the experimental setup described in the previous section is the use of an 8^o directional/hemispherical integrating sphere mounted above the scatterometer sample stage position. This integrating sphere is shown in Fig 11. The silicon photodiode detector was fixed to one port of the sphere. The dependence of the hemispherical reflectance versus receiver power is fitted using a third-degree polynomial regression:

$$R(P) = A + BP - CP^2 + DP^3 \quad (6)$$

The coefficients of the polynomial can be calculated by fitting the receiver power measured using a set of 7 gray Spectralon standard plates with known 8^o directional/hemispherical reflectance. With the setup described above, the power was measured at each wavelength of interest for each standard plate and the coefficients were calculated using MathCAD 3^{rd} degree polynomial fitting procedure. The coefficients calculated are given in Table 1. To verify the proposed procedure the distribution of the difference between the Labsphere measured and our measured 8^o directional/hemispherical reflectance values of the Spectralon samples of nominal reflectance 5%, 10%, 20%, 40%, 60%, 80% and 99% are shown in Fig. 12 for the spectral range 300-900 nm. The measured 8^o directional/hemispherical data of JSC Mars-1 are given in Table 2.

CONCLUSIONS

The BRDF and 8 degree hemispherical reflectance of Martian regolith simulant JSC Mars-1 were measured using the scatterometer located in NASA's GSFC DCaF. A monochromator-based light source in the UV, VIS and NIR spectral regions for both BRDF and hemispherical measurements was employed. In-plane and out-of-plane geometries were used for the BRDF measurements at a number of incident angles of incidence and over a range of scatter angles. The experimental data show a flat BRDF response in the UV with increasing deviation from the Lambertian at higher wavelengths. The ferric absorption feature in the 800-900 nm spectral region is evident in the BRDF versus wavelength data. The 8^o directional/hemispherical data support the spectral distribution data from the BRDF measurements. The hemispherical and diffuse scatter data obtained from these studies are important for future Mars space and ground based

observations through analysis of its diffuse reflectance properties. The BRDF of the sample varies widely depending on angles of incidence and scatter. The reported data were measured in clean room calibration facility and the results presented are NIST traceable trough calibrated standard plates.

REFERENCES

1. T.F. Schiff, M.W. Knighton, D.J. Wilson, F.M. Cady, J.C. Stover, and J.J. Butler, "A Design Review of a High Accuracy UV to Near Infrared Scatterometer", Proc. SPIE, 1995, 121-130 (1993).

2. J.R. Proctor and P.Y. Barnes, "NIST High accuracy reference reflectometer - spectrophotometer", J. Res. Nat. Inst. Stand. Technol., 101, 619-627, (1996).

3. C.C. Allen, R.V. Morris, K.M. Jager, D.C. Golden, D.J. Lindstrom, "Martian Regolith Simulant JSC Mars-1", Lunar and Planetary Science XXIX, Paper #1954 (1998)

4. F.E. Nicodemus, J.C. Richmond, J.J. Hsia, I.W. Ginsburg, and T. Limperis, "Geometrical considerations and nomenclature for reflectance", National Bureau of Standards, NBS monograph 160, Oct. 1977

5. J.C. Stover, "Optical scattering: measurement and analysis" 1995

6. B.N. Taylor and C. E. Kuyatt, "A Guidelines for Evaluating and Expressing the Uncertainty of NIST Measurement Results", NIST Technical Note 1297, U.S. Department of Commerce, National Institute of Standards and Technology, Sep. 1997.

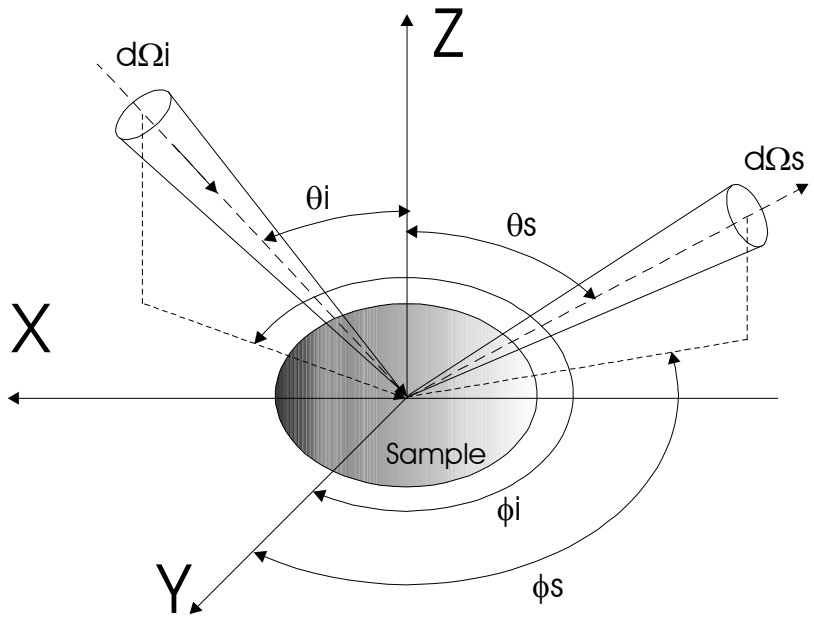

Fig.1 Defining the BRDF in terms of usually adopted symbols

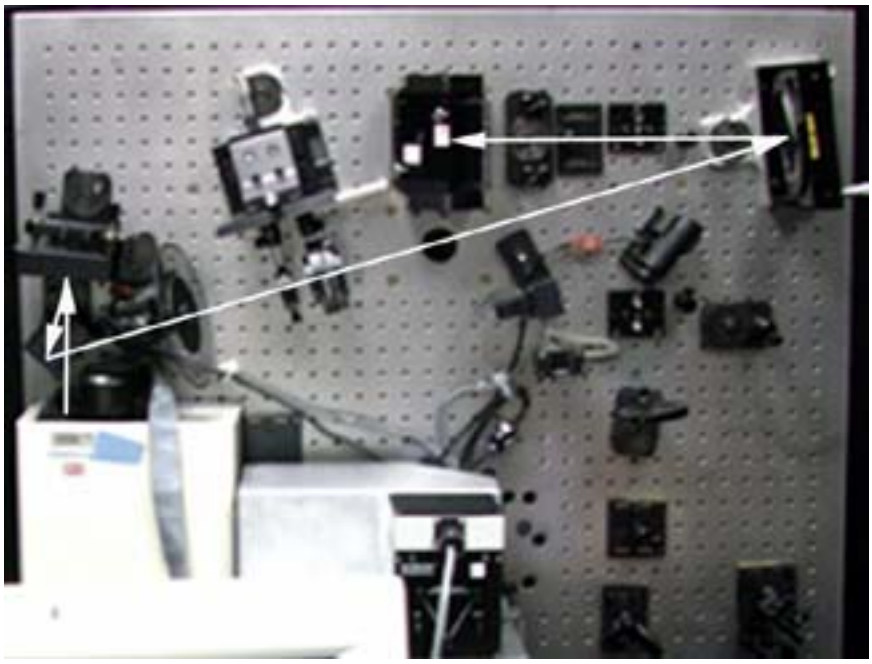

Fig.2 Optical setup of the Scatterometer

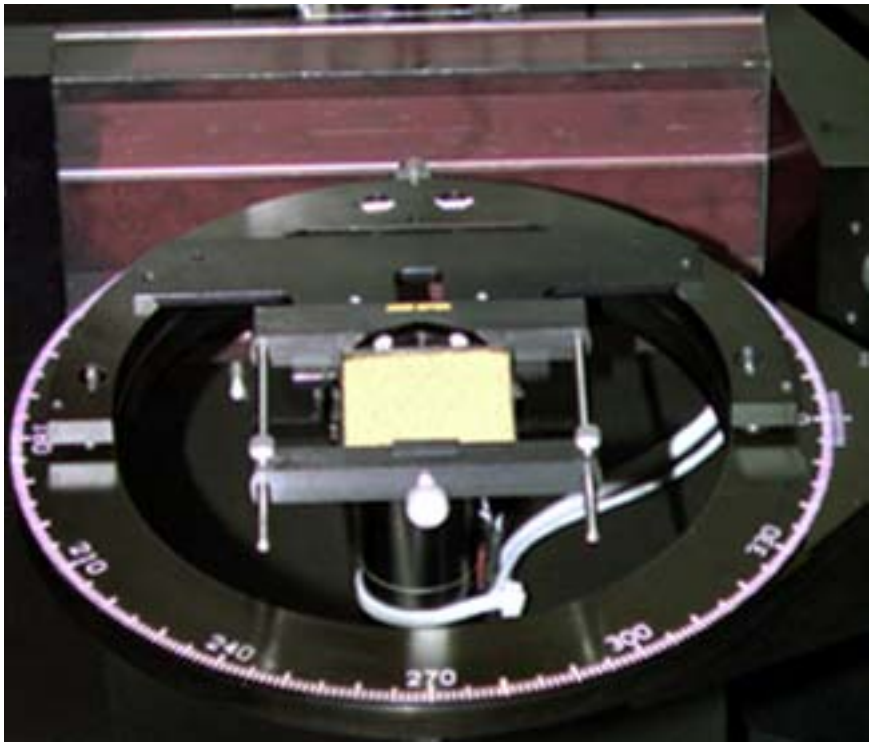

Fig.3: JSC Mars-1 sample fixed on the sample stage

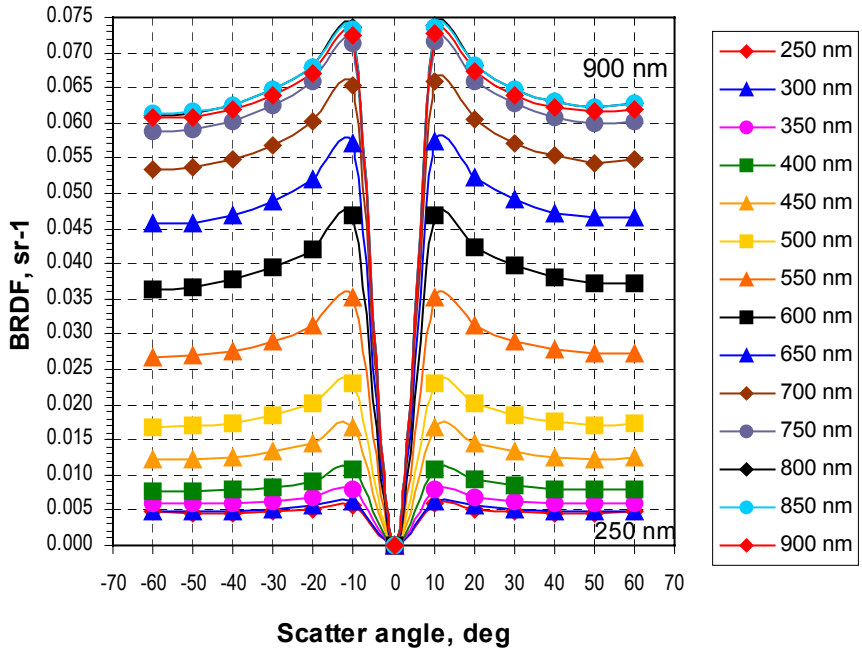

Fig.4: BRDF at normal incidence, in-plane

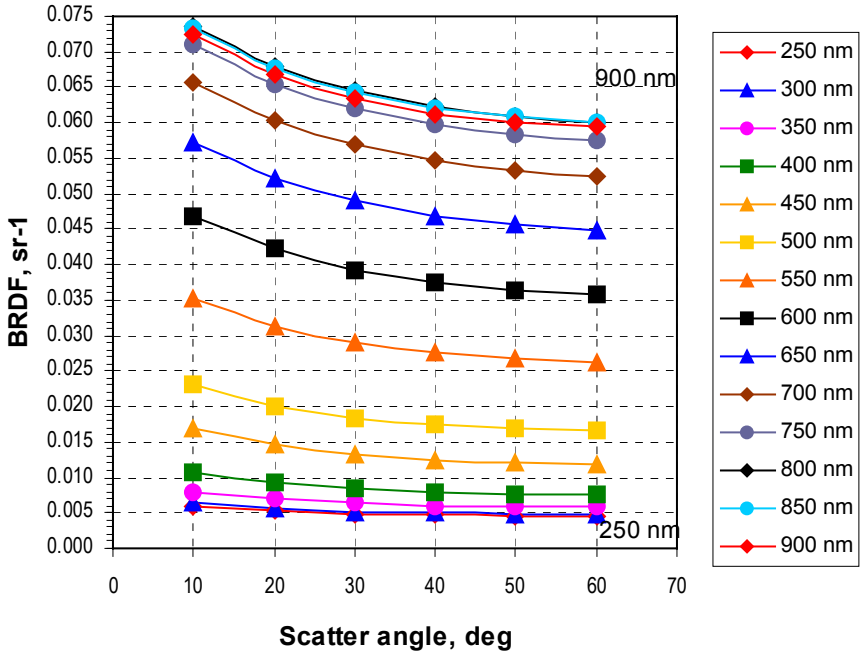

Fig.5: BRDF at normal incidence, out-of-plane

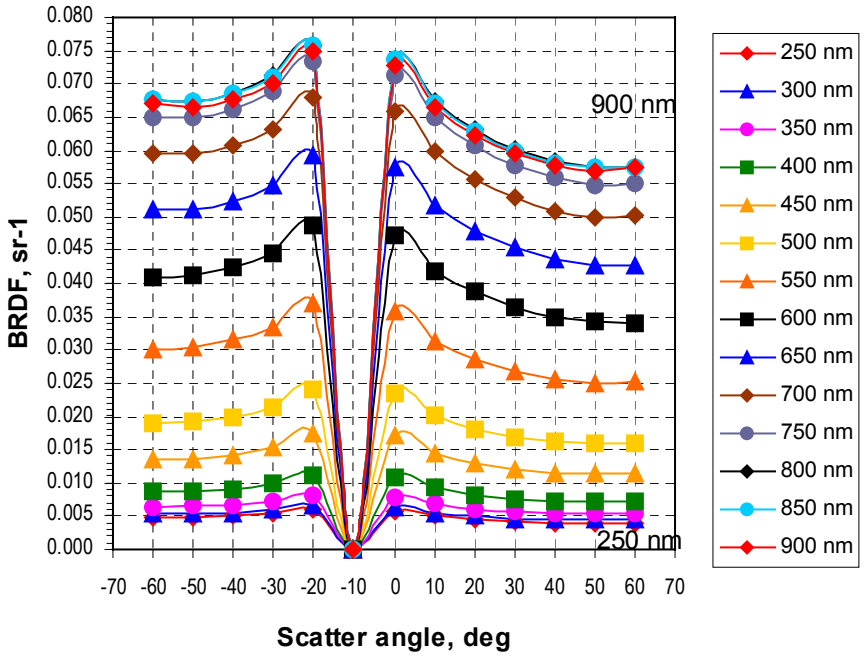

Fig.6: BRDF at 10^{o} incidence, in-plane

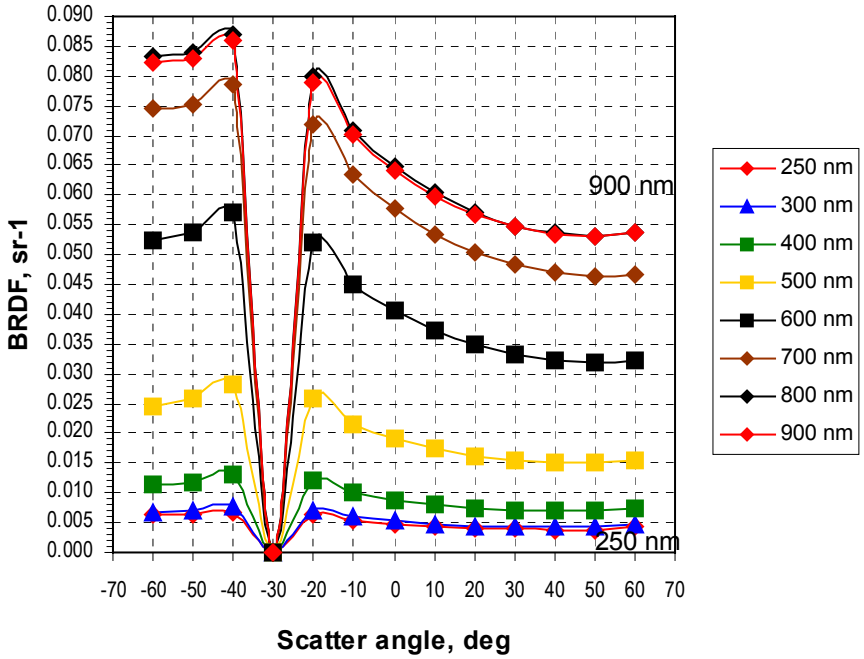

Fig.7: BRDF at 30^{o} incidence, in-plane

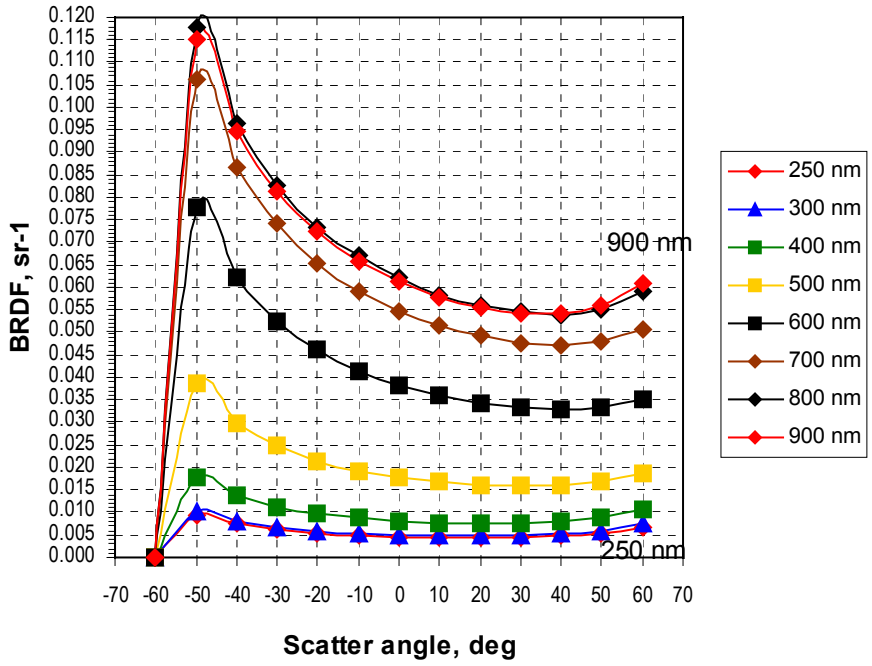

Fig.8: BRDF at 60° incidence, in-plane

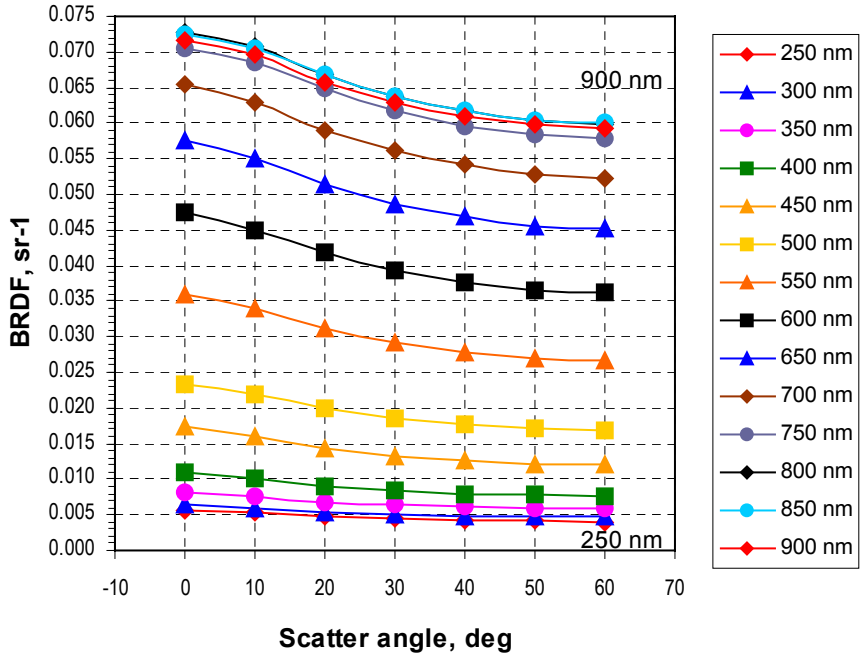

Fig.9: BRDF at 10° incidence, out-of-plane

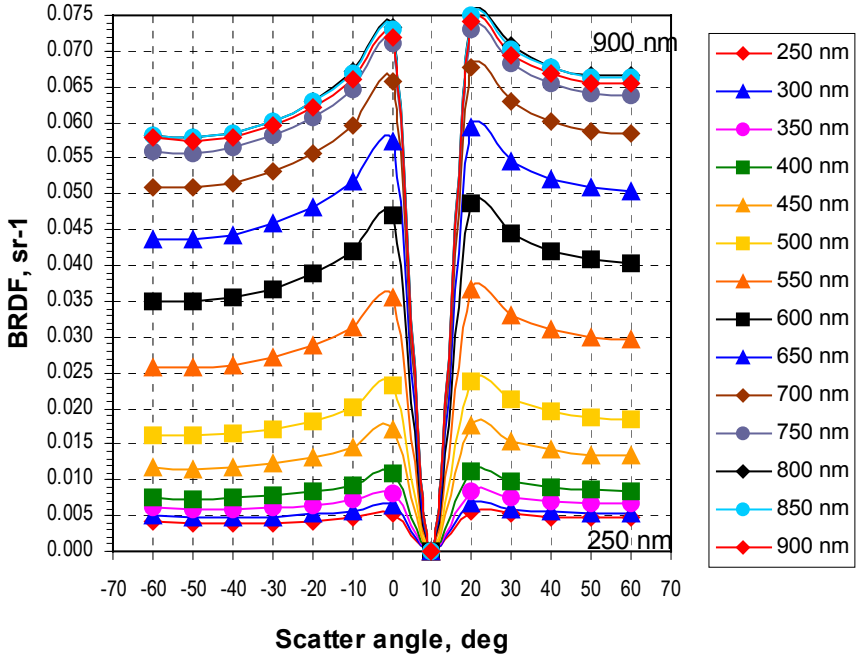

Fig.10: BRDF at -10^{o} incidence, in-plane

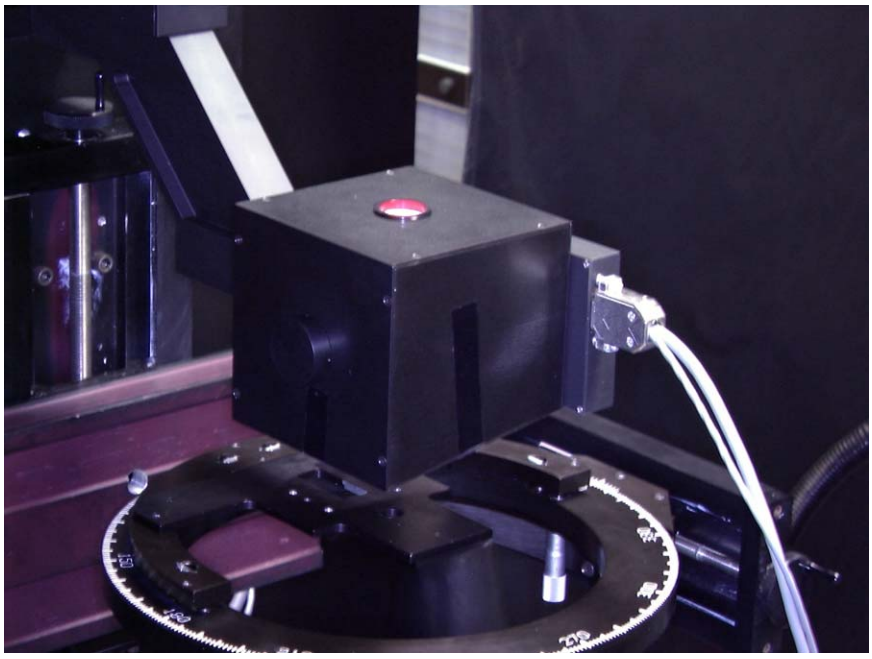

Fig.11: 8 directional/hemispherical reflectance integrating adapter attached to the Scatterometer.

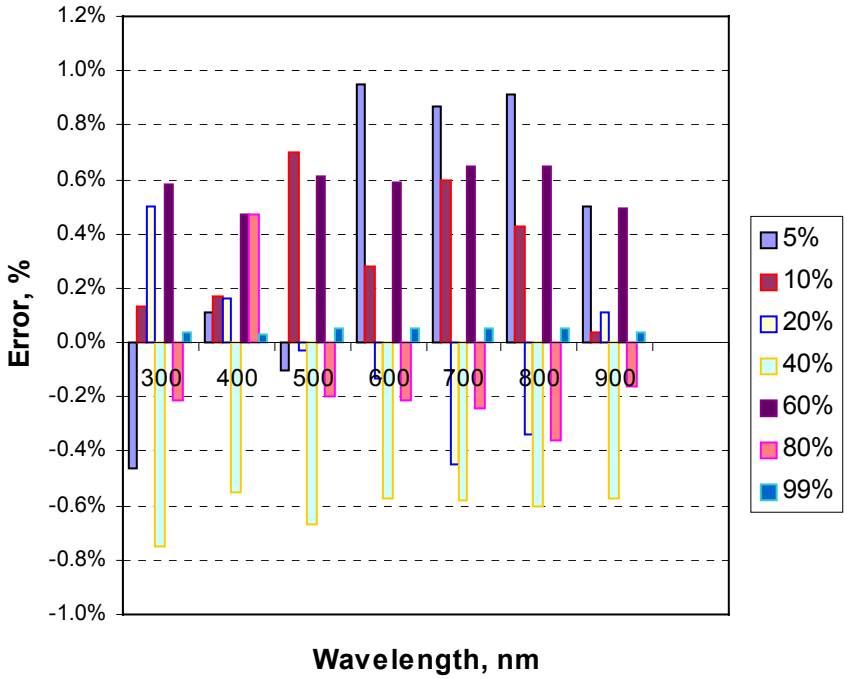

Fig.12: Difference between standard and measured values for the set of 7 Spectralon plates.

Table 1: Polynomial coefficients

Wavelength, nm	A	B	C	D
300	-9.82894×10^{-4}	0.29122	-0.02605	1.66337×10^{-3}
400	3.40319×10^{-3}	1.19252	-0.45747	0.10296
500	4.0201×10^{-3}	0.34171	-0.03957	2.58476×10^{-3}
600	4.90461×10^{-3}	0.38612	-0.05035	3.61316×10^{-3}
700	5.70006×10^{-3}	0.56125	-0.10729	0.01139
800	6.15911×10^{-3}	1.03389	-0.36472	0.07069
900	4.33566×10^{-3}	0.1615	-8.66674×10^{-3}	2.43788×10^{-4}

Table 2: 8 degree hemispherical reflectance of JSC Mars-1

Wavelength, nm	Hemispherical Reflectance
300	0.04269
400	0.02798
500	0.05093
600	0.10187
700	0.14445
800	0.1623
900	0.15908